Eur Radiol (2007) 17: 1135–1146
DOI 10.1007/s00330-006-0453-5

Thomas M. Link
Robert Stahl
Klaus Woertler

Cartilage imaging: motivation, techniques, current and future significance

Received: 3 May 2006
Revised: 1 August 2006
Accepted: 22 August 2006
Published online: 9 November 2006

T. M. Link (✉) · R. Stahl
Department of Radiology,
University of California,
400 Parnassus Ave, A-367,
San Francisco, CA 94143, USA
e-mail: tmlink@radiology.ucsf.edu
Tel.: +1-415-3532450/8940
Fax: +1-415-4760616

K. Woertler
Institut für Röntgendiagnostik des
Klinikums rechts der Isar,
Technische Universität München,
München, Germany

Abstract Cartilage repair techniques and pharmacological therapies are currently areas of major clinical interest and research, in particular to prevent and treat osteoarthritis. MR imaging-based techniques to visualize cartilage are prerequisites to guide and monitor these therapies. In this review article, standard MR imaging sequences are described, including proton density-weighted fast spin echo, spoiled gradient echo and dual echo steady state sequences. In addition, new sequences that have been developed and are currently being investigated are presented, including driven equilibrium Fourier transform and steady-state free precession-based imaging. Using high-field MR imaging at 3.0-T, visualization of cartilage and the related pathology has been improved. Volumetric quantitative cartilage MR imaging was developed as a tool to monitor the progression of osteoarthritis and to evaluate new pharmacological cartilage protective therapies. The most exciting developments, however, are in the field of cartilage matrix assessment with quantitative dGEMRIC, T2 and T1rho mapping techniques. These techniques aim at detecting cartilage damage at a stage when changes are potentially still reversible, before cartilage tissue is lost. There is currently substantial interest in these techniques from rheumatologists and orthopedists; radiologists therefore need to keep up with these developments.

Keywords Cartilage · Cartilage repair · Cartilage volume · MR imaging · MR sequences · Quantitative MR imaging

Motivation to optimize cartilage imaging

Cartilage is one of the most important biomarkers in degenerative and traumatic joint disease. MR imaging has been established as the standard cartilage imaging modality, and techniques have been developed and optimized (1) to visualize cartilage morphology, (2) to quantify its volume and (3) to analyze its biochemical composition. The substantial amount of research that is invested in the development of these morphologic and quantitative imaging techniques is motivated by new therapeutic modalities both on a surgical (cartilage repair) and a pharmacological level.

What therapies are available?

New surgical techniques that are available to treat focal cartilage lesions include mosaicplasty, microfracture, drilling procedures and autologous chondrocyte implantation [1–3]. Mosaicplasty, also termed osteochondral autograft transplantation (OAT) or autologous osteochondral transplantation, is one of the most promising techniques that has been developed [4–6]. This technique is used most frequently at the knee and ankle joints, but has also been advocated in other joints such as the elbow to treat focal chondral or osteochondral defects due to injury, degeneration, osteochondritis dissecans or osteonecrosis. In the

microfracture technique, small perforations are created in the subchondral bone plate after debridement of a cartilage defect. Drilling procedures are applied in osteochondritis dissecans if the cartilage surface is intact, but they are frequently only successful if patients are skeletally immature [7]. Chondrocyte implantation has been performed with autologous chondrocytes and allografts. The cartilage defect is debrided and filled with a suspension of cultured chondrocytes and covererd by a periosteal flap or chondrocyte-impregnated scaffolds [8]. The results are somewhat controversial [9, 10], with one study indicating that cartilage repair tissue was of varying morphology ranging from predominantly hyaline in 22% of biopsy specimens, to mixed in 48%, and to predominantly fibrocartilage in 30% [10]. A recent study [11] comparing mosaicplasty and autologous chondrocyte implantation showed that both treatments resulted in a decrease in patient symptoms. However, the improvement provided by the autologous chondrocyte implantation lagged behind that provided by mosaicplasty. Histologically, the defects treated with autologous chondrocyte implantation were primarily filled with fibrocartilage, whereas the osteochondral cylinder transplants retained their hyaline character.

A number of pharmacological therapies have been suggested to preserve cartilage or to treat cartilage damage. These include (1) injectable therapies, such as corticosteroids and viscosupplementation that have elicited a favorable short-term response, but no long-term structural modification, and (2) slow-acting drugs, such as chondroitin and glucosamine sulfate, which have shown promising results [12]. Anti-inflammatory activity and the chondroprotective action of chondroitin sulfate associated with modifying cartilage structure have been found [13]. Pharmaceutical companies are currently investing forcefully in developing cartilage protective agents, which will be available in the near future. These are also driving the research in developing MR-based biomarkers to assess protective effects of their agents at the earliest possible stage.

What are the indications for cartilage imaging?

The most important clinical indications for MR imaging are the assessment of cartilage in osteoarthritis, chronic or acute osteochondral injury, osteochondritis dissecans, chondromalacia patellae, spontaneous osteonecrosis of the femoral condyle (SONC or Ahlbaeck's disease) and inflammatory arthropathies (in particular before invasive therapy). In addition, dedicated cartilage imaging is required after invasive cartilage repair procedures or conservative therapies, including pharmacological therapies, to monitor the treatment's effect. MR studies are required to tailor therapies, and in the future, new quantitative techniques may at some stage have significance in indicating treatment as well as monitoring therapy similar to the bone mineral density currently used in the setting of osteoporosis.

What are the standard sequences to image cartilage?

Most experience and good results in imaging cartilage and chondral pathology were gathered with (1) proton-density (PD) and T2-weighted (w) fast spinecho (FSE) and (2) 3D spoiled gradient echo (SPGR) or fast low-angle shot (FLASH) sequences. Additional fat suppression in these sequences was found useful to visualize cartilage pathology. While 3D SPGR and FLASH sequences are well suited to depict surface lesions, PD-w and T2-w FSE sequences also show cartilage internal pathology because of the more intermediate signal of the cartilage and higher intrinsic cartilage contrast in these sequences (Fig. 1). Many institutions, including those of the authors, tend to use intermediate-w FSE sequences with a mixed PD/T2 contrast (echo time =33–60 ms), which are thought to provide higher intrinsic contrast and to be less prone to magic angle effects as compared with "true" PD-w pulse sequences obtained at short echo times. The bright signal in the SPGR and FLASH images limits visualization of internal cartilage pathology to

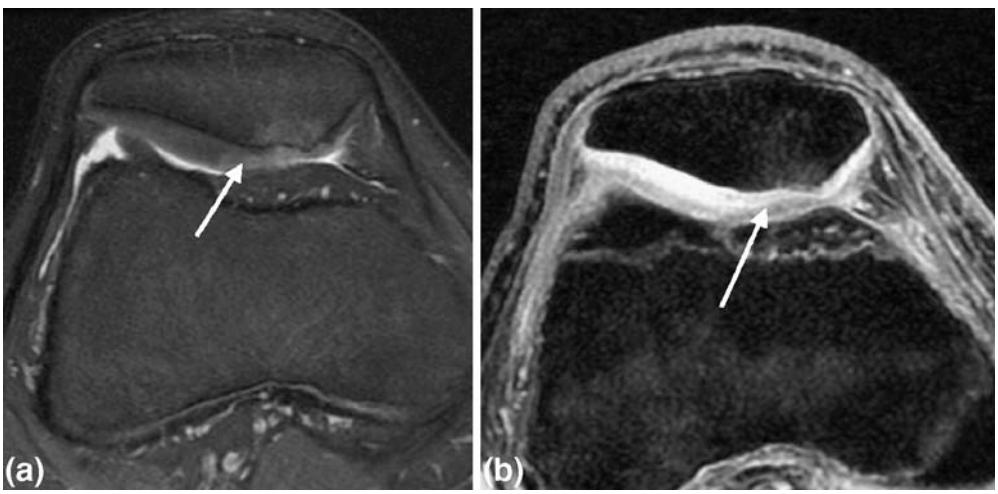

Fig. 1 Chondromalacia patellae in a 19-year-old male patient. A fs intermediate-w FSE (4,300/51 ms; TR/TE) (**a**) and a fs T1-w SPGR (21/12.5 ms/15 degrees; TR/TE/flip angle) (**b**) sequence were obtained in an axial orientation at 3.0 T. Cartilage defects and edema as well as subchondral bone edema are shown. Note that the intermediate-w FSE sequence shows increased signal of cartilage clearly (*arrow* in **a**), while SPGR sequence shows better delineation of cartilage surface (*arrow* in **b**)

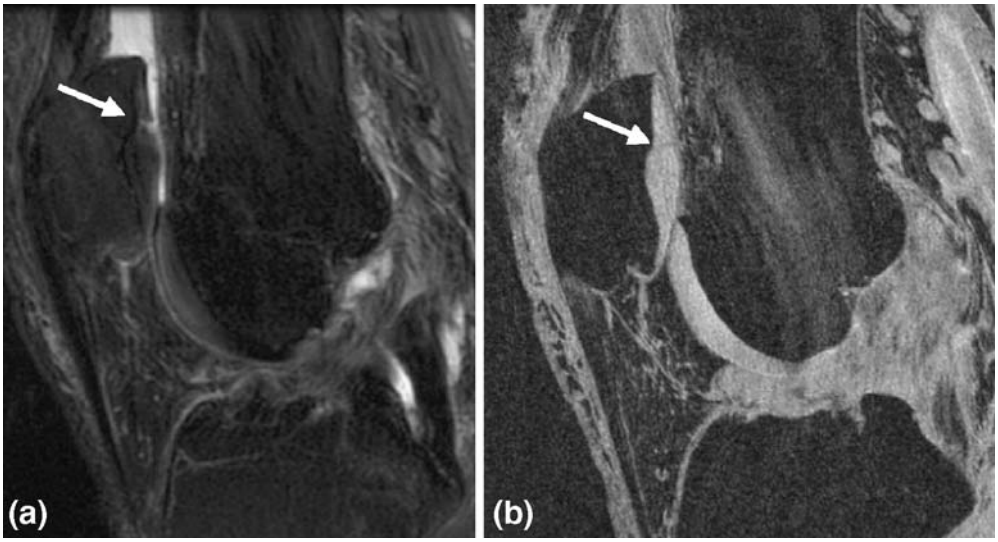

Fig. 2 Cartilage fissure (*arrows*) in a 45-year-old female imaged with a fs intermediate-w FSE (4,300/51 ms) (**a**) and a fs T1-w SPGR (21/12.5 ms/15 degrees) (**b**) sequence obtained in a sagittal orientation. Note that the fissure is clearly depicted with the intermediate-w FSE image, while it is not as well appreciated on the fs SPGR image. Popliteal artery pulsation artifacts are more pronounced on the SPGR sequence

some extent, and fissures, for example, may sometimes be not as well visualized (Fig. 2). A number of studies have been performed comparing SPGR versus PD or T2-w FSE sequences [14–16], and similar overall diagnostic performance in detecting focal cartilage lesions has been found for both sequence types. 3D SPGR and FLASH sequences provide high spatial resolution; however, imaging time with these sequences is usually fairly high, and image quality can be degraded by motion artifacts. These gradient echo sequences are also very sensitive to susceptibility artifacts, which should be considered after previous surgery, in particular after cartilage repair procedures. In our clinical practice, we found intermediate–w FSE sequences (the acquisition time of high-resolution sequences was approximately 7–12 min) easier to use and more practically applicable than SPGR or FLASH (acquisition time approximately 9–14 min) sequences. Bredella et al. [17] also found these sequences to be accurate and fast for detecting and grading articular cartilage defects in the knee. In their experience, a combination of different planes improved the sensitivity and specificity for chondral defects.

In addition to these sequences, the 3D double echo steady state sequence (3D DESS) has also shown good results in detecting cartilage lesions (Fig. 3). This mixed T1/T2*-w sequence provides high spatial resolutions with the cartilage appearing more intermediate in signal. In an experimental study, Woertler et al. [18] found a similar performance of fs 3D FLASH and water-excited 3D double-echo steady state (DESS) sequences in detecting cartilage surface lesions. Ruehm et al. analyzed patellar cartilage abnormalities in 58 consecutive patients using a 3D-DESS without fat suppression and a T2-weighted FSE sequence. These authors concluded that the DESS sequence was less accurate in detecting cartilage surface abnormalities, yet more accurate in diagnosing cartilage softening [19].

What field strength should be used to image cartilage?

This question is easily answered with regard to the clinically available systems: the higher the field strength, the better the diagnostic outcome. At present, standard imaging is performed at 1.5 T, as 3-T systems are not yet widely available. Low-field systems should not be used for cartilage imaging as previous studies have shown that low-field MR scanners operating at field strengths of 0.18–0.20 T [18, 20, 21] have substantial limitations

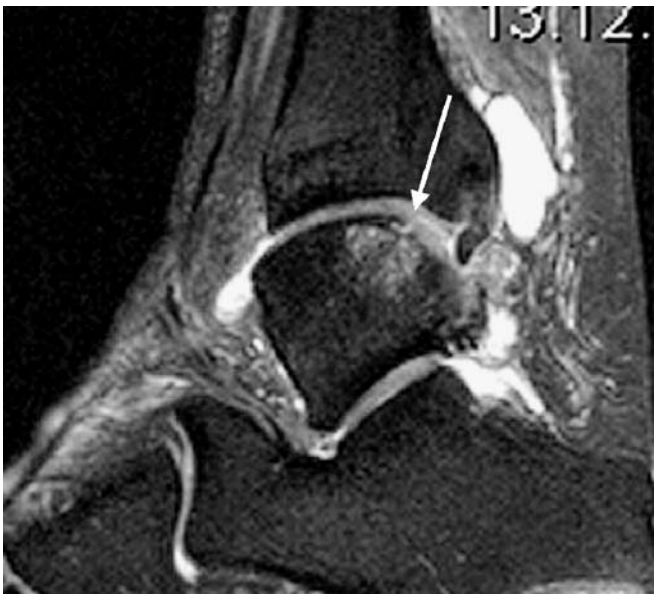

Fig. 3 DESS sequence (25.7/9 ms) with water excitation obtained in a sagittal orientation at the ankle in a 30-year-old male with an acute trauma. A cartilage fissure at the talus (*arrow*) and adjacent bone marrow edema are visualized. Note that cartilage is intermediate in signal, while joint fluid is bright

compared to high-field systems (1.5 T) in visualizing cartilage pathology.

As previously mentioned, 3-T systems have shown promise in optimizing cartilage imaging. The great appeal of 3-T MR imaging for musculoskeletal MR is the improvement in image quality and spatial resolution. Because the signal-to-noise ratio (SNR) correlates in an approximately linear fashion with field strength, it is roughly twice as great at 3 T as at 1.5 T. The time necessary to acquire satisfactory images can be substantially reduced, minimizing motion artifacts and possibly speeding patient turnover. Alternatively, the same acquisition time can be used to obtain images at higher spatial resolution. Also, greater contrast is available at higher field strength. All of these features are particularly attractive for cartilage imaging, in particular for smaller joints. However, acquisition of imaging studies with a higher field machine clearly mandates considerable adjustment of an MR imaging practice, including revision of many imaging protocols. We have to be aware of the fact that greater SNR and contrast come at a price. First, tissues differ in their magnetic susceptibility, and this effect is exacerbated at higher field strengths. Second, there are safety concerns: the energy deposited in the patient's tissues is fourfold higher at 3 T than at 1.5 T. Third, 3-T images are more subject to flow artifacts, which may be a particular problem in the knee joint. In addition there is doubling of the chemical shift when the field strength is doubled. Imaging parameters therefore have to be adjusted to the higher field strength, which includes increasing TR and bandwidth as well as decreasing TE and flip angles [22–24].

Previous in vitro studies showed that artificial defects created in specimens were better visualized at 3 T than at 1.5 T [14, 15, 25]. Figure 4 shows representative images obtained at 1.5 T (a) and at 3 T (b) with a fat saturated PD w imaging sequence and identical acquisition times. Similar results were also obtained in vivo [26]. Figure 5 shows sagittal images of the knee joint in a subject with an osteochondral lesion at the femoral condyle obtained with a SPGR sequence obtained with the same acquisition time at 1.5 and 3 T. The differences in image quality and SNR are clearly appreciated.

What new techniques are available to image cartilage?

A number of sequences have been developed to improve morphological depiction of cartilage. These include driven equilibrium Fourier transform (DEFT) and steady-state free precision (SSFP) imaging.

DEFT imaging makes use of a much higher cartilage-to-fluid contrast; the signal of synovial fluid is higher than in SPGR sequences, and the signal of cartilage is higher than in T2-ws FSE sequences [27]. Yoshioka et al. used this sequence in 35 osteoarthritic knees and correlated the imaging findings with arthroscopy; in their study, the fat-suppressed three-dimensional DEFT images showed results similar to SPGR and PD-w FSE sequences with high sensitivities yet relatively low specificities [16]. Gold et al. compared 3D-DEFT and T2-FSE sequences in 104 consecutive patients with knee pain and used arthroscopy in 24 patients as a standard of reference [28]. These investigators found that the 3D-DEFT sequences provided excellent synovial fluid-to-cartilage contrast while preserving signal from cartilage, giving this method a high cartilage SNR. In addition, 3D-DEFT showed the full cartilage thickness better than T2-FSE, yet T2-FSE had superior fat saturation and fewer artifacts than 3D-DEFT.

SSFP imaging has been described as an efficient, high-signal method for obtaining 3D images and may be useful to depict cartilage since cartilage signal was found to be higher than in conventional sequences [29]. Kornaat et al. used this sequence in volunteers at 1.5 and 3 T and found that SSFP-based techniques showed a higher increase in SNR and CNR efficiency at 3 T than SPGR sequences [26]. Figure 6 shows a representative image of a knee joint with

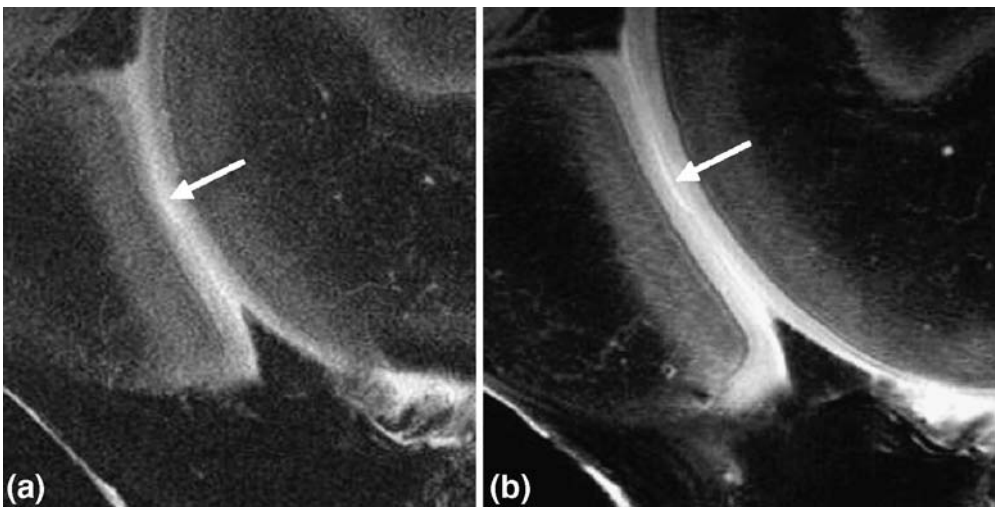

Fig. 4 Artificially created cartilage lesion at the patella (*arrows*) in a pig knee imaged with a fs intermediate-w FSE at 1.5 T (**a**) and 3.0 T (**b**) (4,000/35 ms). Note that the lesion is substantially better visualized at 3.0 T

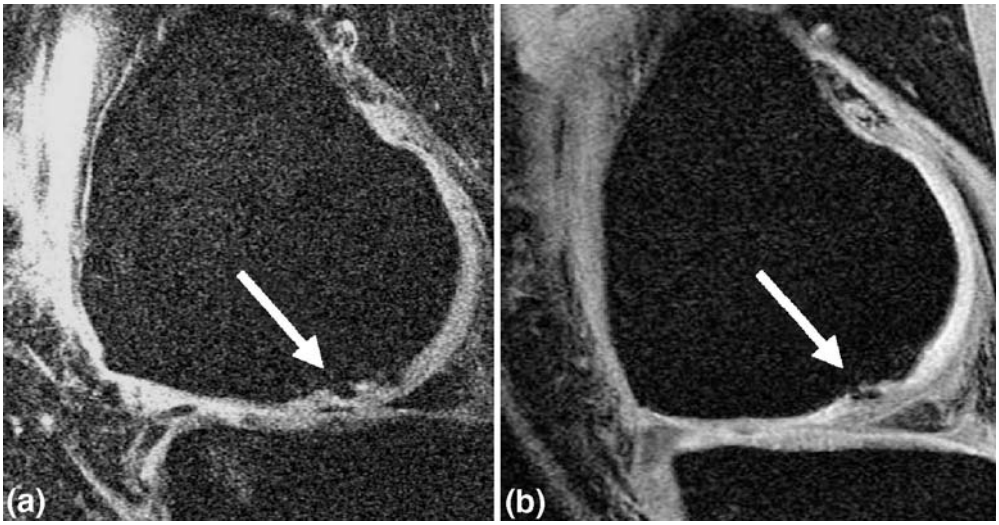

Fig. 5 Osteochondral lesion in a 32-year-old male with chronic knee pain. Sagittal SPGR sequences obtained at 3.0 T (21/12.5 ms/15 degrees) (**b**) and at 1.5 T (30/16 ms/30 degrees) (**a**) with similar acquisition times. Note that image quality is substantially improved at 3.0 T and the lesion (*arrows*) is substantially better visualized at 3.0 T

cartilage defects at the posterior medial femoral condyle imaged with a non-fat saturated SSFP sequence. Bauer et al. compared SSFP, PD-w FSE and SPGR sequences in their performance in assessing cartilage lesions at cadaver ankles and found the highest ROC (receiver-operator characteristics) values for PD-w FSE sequences at 3.0 T, yet FSE and SSFP sequences showed a similar performance at 1.5 T, and both showed better results at 3.0 and 1.5 T than the SPGR sequence [22]. To our knowledge, larger clinical studies, however, have not yet been performed using this sequence. It should be noted that the previously described DESS sequence is also a steady state sequence and thus has cartilage signal features similar to the SSFP sequences, yet the parameters are different to some extent.

Direct MR arthrography with the use of T1-weighted pulse sequences following the intraarticular injection of gadolinium chelates has been shown to represent a reliable imaging technique for the detection of surface lesions of articular cartilage with sensitivities and specificities ranging from 85 to 100% [30, 31]. The injected fluid produces high contrast within the joint space, and at the same time distends the joint, and thus improves the separation of corresponding joint surfaces, such as the chondral surfaces of the femur and the tibia. A simple method to produce artificial arthrographic contrast in a T1-like FSE sequence with the use of a driven equilibrium pulse (DRIVE) has recently been described (Fig. 7). In contrast to the 3D DEFT sequence mentioned above, this 2D technique provides bright signal intensity of joint fluid with otherwise unchanged signal intensities compared with a normal T1-w FSE sequence at high spatial resolution and short scan times [32]. Driven equilibrium pulses can also be used to increase the contrast and/or spatial resolution of intermediate weighted FSE images (Fig. 8). However, this new technique and its value for cartilage imaging are still under clinical evaluation.

The role of cartilage volume

Quantitative MR imaging of cartilage is currently used in ongoing studies to monitor cartilage volume and will be used to assess structural effects of pharmacological therapies on cartilage in order to prove their effectiveness (Fig. 9). Although joint space narrowing on weight-bearing radiographs still is the accepted surrogate marker for demonstrating structural change by regulatory agencies, this is expected to change in the near future, given the

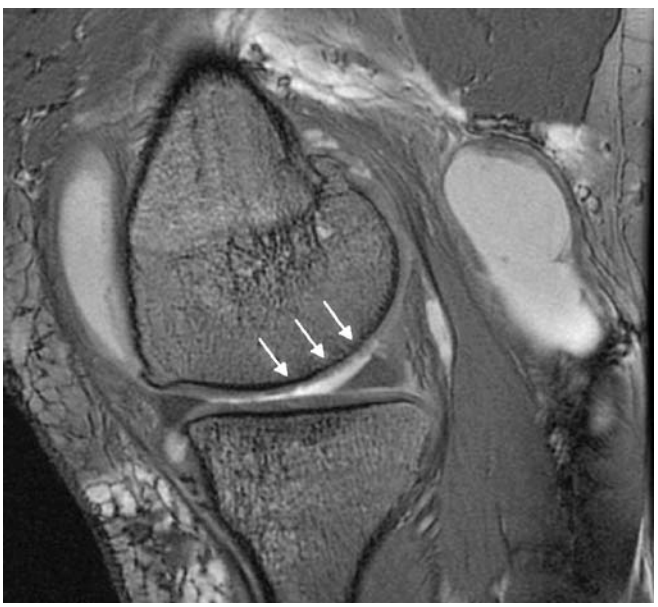

Fig. 6 Sagittal MR image in a patient with osteoarthritis and extensive cartilage lesions at the medial femoral condyle of the knee joint (*arrows*). The image was obtained with a SSFP sequence (5.5/1.9 ms/15 degrees) without fat saturation. Cartilage is intermediate to low in signal and fluid is bright; note large joint effusion and baker cyst as well as osteophytes

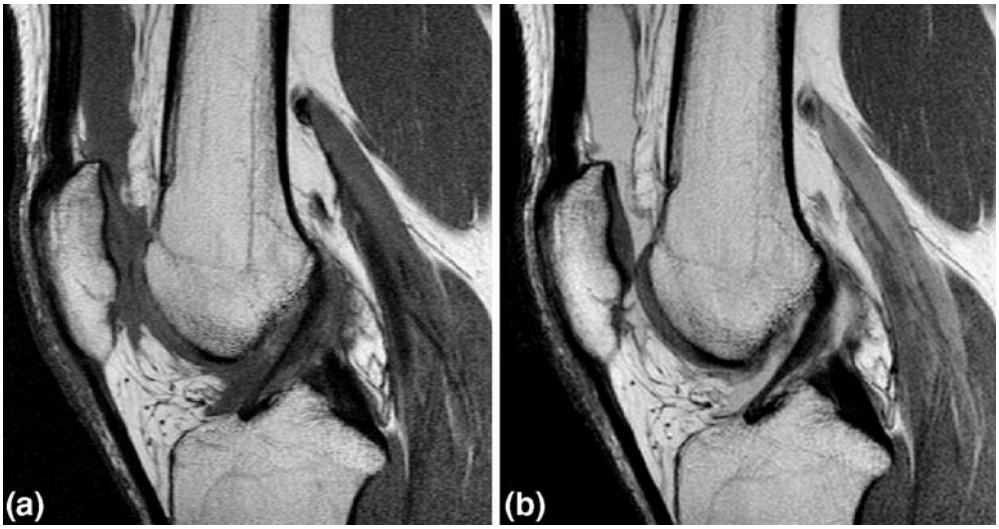

Fig. 7 Native arthrographic effect of a driven equilibrium pulse. Sagittal T1-weighted FSE image (600/20 ms) (**a**) and corresponding FSE image (600/20 ms) with driven equilibrium pulse (**b**) shows increase of signal intensity of free water resulting in bright signal of joint fluid with otherwise unchanged signal intensities

inherent limitations of radiography. Considering the tremendous cost involved to bring a drug to market and the limited time during which a drug can be exclusively marketed by the company who has developed it, it is evident that a decrease in the study duration and/or study participants involves huge economic savings for the pharmaceutical industry, and this has stimulated high interest in this novel technology. Quantitative MR imaging of cartilage is also used in the Osteoarthritis Initiative (OAI), a current program jointly sponsored by the National Institute of Arthritis and Musculoskeletal and Skin Diseases (NIAMS) of the National Institute of Health (NIH) and the pharmaceutical industry targeted at iden-

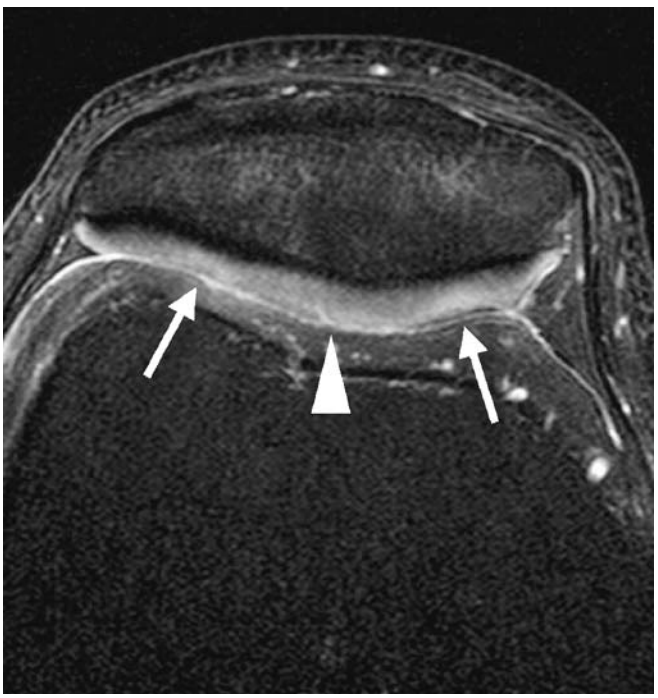

Fig. 8 High resolution intermediate weighted FSE image with driven equilibrium pulse obtained at 1.5 T shows areas of increased signal intensity (*arrows*) as well as superficial fissuring (*arrowhead*) of patellar cartilage consistent with grade 1 (softening/swelling with intact cartilage surface) and 2 (fissuring/blistering) articular cartilage lesions

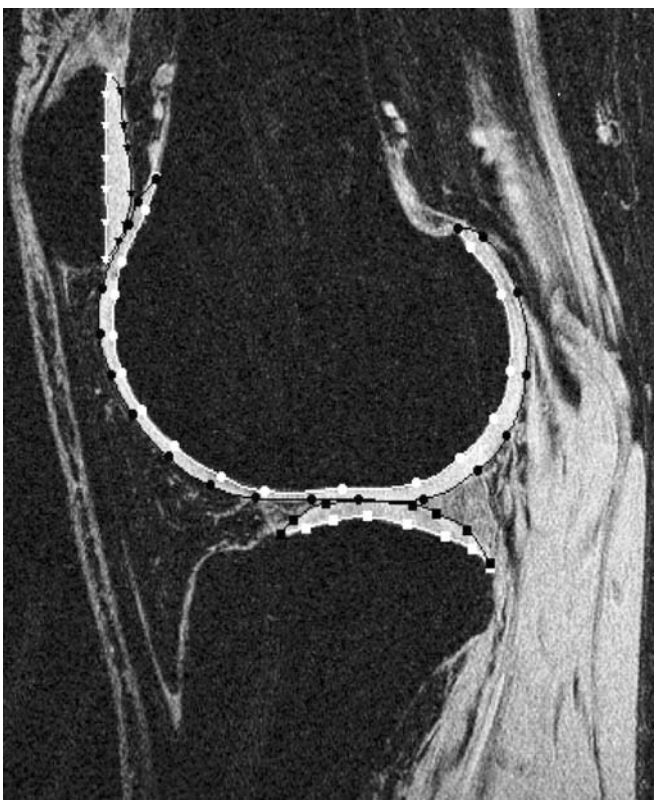

Fig. 9 Segmentation of femoral (•), tibial (▪), and patellar (▾) cartilage on a sagittal SPGR image using a semi-automatic technique based on Bezier-Splines and edge-detection. Bone-cartilage interface: *white line*: articular surface: *black line*

tifying the most promising OA biomarkers for analyzing the development and progression of symptomatic knee osteoarthritis involving a cohort of 5,000 participants that will be imaged for a period of 5 years. Also, a number of clinical, longitudinal studies found that quantitative MR imaging could measure the progression of knee OA precisely and help to identify patients with rapidly progressing disease [33–35].

Considerable effort has been spent on optimizing cartilage volume measurements to serve as potential outcome markers in pharmaceutical trials. The MR sequences that have been almost exclusively used for cartilage morphology quantification are thin section fs T1-wSPGR or FLASH sequences. With these images, cartilage displays higher signal in comparison with adjacent tissues (bone and joint fluid), facilitating segmentation of the cartilage (Fig. 9). Several semi-automated techniques have been described to optimize cartilage segmentation, including active shape models, edge detection, fitting B-splines to manually segmented points and B-spline snake (active contours) [36–38], but to date, most large-scale studies have relied on manual segmentation.

Eckstein et al. found long-term precision errors that ranged from 1.4% (total knee) to 3.9% (total femur) for cartilage volume and thickness [39], making this technique attractive for longitudinal studies. It was also shown that noninvasive quantitative MR imaging-based analysis of cartilage morphometry is accurate and precise in severe OA and displays high potential diagnostic value [40]. Quantitative analysis of OA by MR imaging using T and Z scores for cartilage volume has been proposed [41]. However, cartilage volume should be normalized to the individual joint surface area in order to maximize the discriminatory power of this technique for the diagnosis of OA.

A recent study found that quantitative MR imaging measurements of cartilage at 3.0 T tended to be more reproducible than at 1.5 T and thus may provide a superior ability to detect changes in cartilage status over time and to determine responses to treatment with structure-modifying drugs [42]. Moreover, Bauer et al. found in an vitro study that measurements of cartilage volume at 3.0 T were more accurate than those obtained at 1.5 T [43].

What are the surrogate measures of cartilage composition?

In the last years, significant interest focused on imaging cartilage composition as a potential early marker for degenerative joint disease. Cartilage consists of approximately 70% water, and the remainder predominantly of type II collagen fibers and glycosaminglycans (GAG). These GAG macromolecules contain negative charges that attract sodium ions (NA^{+}). One of the most common MR contrast agents, gadopentetate dimeglumine ($Gd\text{-}DTPA^{2-}$; Magnevist®, Schering, Berlin, Germany), has a negative charge and will therefore show a lower concentration in cartilage areas of high GAG concentrations following penetration via diffusion. In fact, it will be distributed in higher concentrations in areas with lower GAG concentration and thus pathologic cartilage composition. Gadopentetate dimeglumine concentrations in cartilage can be quantified, and this technique has been defined as dGEMRIC or delayed gadolinium-enhanced MR imaging of cartilage. Initial studies have shown that the dGEMRIC measurement of GAG corresponds to the true GAG concentration as measured with biochemistry and histology [44, 45]. This technique has also been used in a number of clinical studies, and variations of this measurement have been shown in patients with osteoarthritis, trials of autologous chondrocyte implants and subjects with sedentary lifestyles versus those with regular exercise [46–49]. Williams et al. examined 31 patients with knee OA using

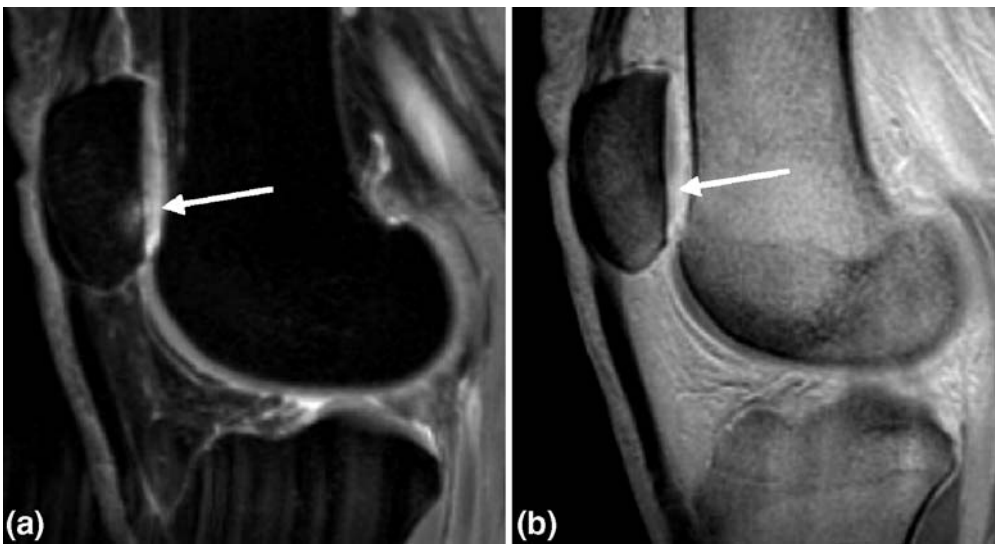

Fig. 10 Sagittal MR images of a 50-year-old female with early osteoarthritis. In (**a**) a fs intermediate-w FSE (4,300/51 ms) sequence shows bone marrow edema at the inferior part of the patella (*arrow*), the overlying cartilage shows subtle signal increase and inhomogeneity. In the contrast-enhanced T1-w dGEMRIC image (**b**) obtained 90-min post-injection increased contrast uptake is shown in the area overlying the area of bone marrow edema (*arrow*) indicating cartilage damage with loss of GAG

MR imaging with a dGEMRIC protocol at 1.5 T as well as semiflexed-knee and full-limb radiographs to assess alignment [49]. These authors found that compartments of the knee joint without joint space narrowing had a higher dGEMRIC index than those with any level of narrowing (mean: 408 ms versus 365 ms; $P=0.001$). In knees with one unnarrowed (spared) and one narrowed (diseased) compartment, the dGEMRIC index was greater in the spared versus the diseased compartment (mean: 395 ms versus 369 ms; $P=0.001$). In spared compartments, there was a trend toward a lower dGEMRIC index with increasing radiographic severity of osteoarthritis. Valgus-aligned knees tended to have lower dGEMRIC values laterally, and varus-aligned knees tended to have lower dGEMRIC values medially. The authors concluded that these quantitative findings may have a particularly important role in evaluating early osteoarthritis. Figure 10 shows images of a patient with early osteoarthritis and patellar cartilage damage as visualized by increased Gd-DTPA uptake in the dGEMRIC study, which is not as well visualized on a standard intermediate-w FSE sequence.

The results of an experimental study with a human patella specimen suggest that delayed imaging can also be useful to diagnose early articular cartilage damage following intraarticular contrast administration (direct MR arthrography) (Fig. 11) [50]. With histopathologic assessment as the standard of reference, delayed T1-weighted MR images allowed the detection of grade 1 (softening/swelling with intact cartilage surface) and 2 (fissuring/blistering) cartilage lesions in 94% of the cases, although the pattern of contrast accumulation within damaged cartilage was somewhat different from that expected from the results of the studies mentioned above. The authors concluded that, at least in cartilage lesions that histologically can already be classified as grade 1 or 2, contrast kinetics might, in addition to the GAG concentration, also be influenced by alterations of the collagen and water content as well as the integrity of the cartilage surface. First results of experimental studies with selectively proteoglycan and collagen depleted cartilage support this theory and indicate that delayed gadolium-enhanced MR imaging might not allow the differentiation of GAG and collagen loss [51].

Another approach that has been used to measure cartilage composition is T2 mapping (Fig. 12). It was shown that the increasing T2 relaxation time was proportional to the distribution of cartilage water and is sensitive to small water content changes [52]. In an early study, Dardzinski et al. examined the spatial variation of in vivo cartilage T2 in young asymptomatic adults and found a reproducible pattern of increasing T2 that was proportional to the known spatial variation in cartilage water and was inversely proportional to the distribution of proteoglycans [53]. These authors postulated that the regional T2 differences were secondary to the restricted mobility of cartilage water within an anisotropic solid matrix. Thus,

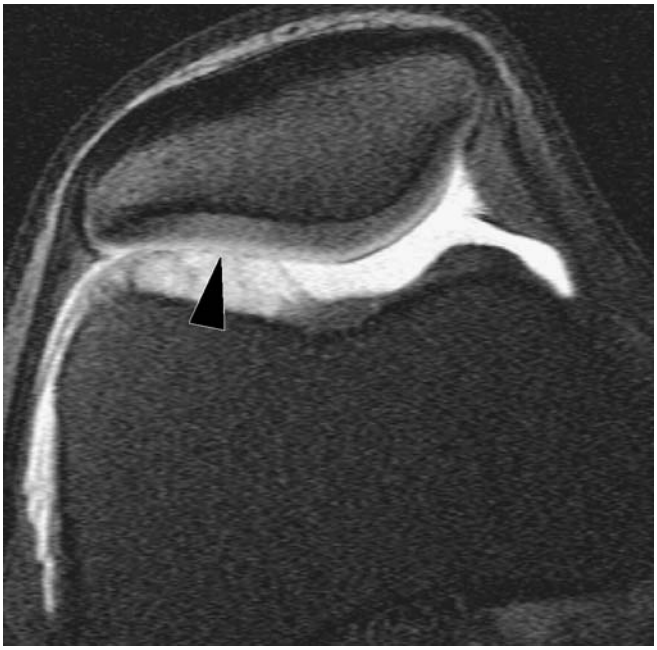

Fig. 11 Delayed transverse fat-suppressed T1-w images obtained after direct MR arthrography show increased contrast uptake of articular cartilage at the lateral facet of the patella (*arrowhead*). Arthroscopy (not shown) verified cartilage softening and the integrity of the cartilage surface consistent with a grade 1 articular cartilage lesion

measurement of the spatial distribution of the T2 reflecting areas of increased and decreased water content may be used to quantify cartilage degeneration before morphologic changes are appreciated.

In a preliminary study, Mosher et al. showed that aging is associated with an asymptomatic increase in T2 of the transitional zone of articular cartilage. The results of their study indicated that this diffuse increase in T2 in senescent cartilage is different in appearance than the focally increased T2 observed in damaged articular cartilage [54]. In an additional study, Mosher et al. obtained T2 maps at 3.0 T of the weight-bearing femoral and tibial articular cartilage in seven young healthy men before and immediately after 30 min of running [55]. They found no statistically significant change in T2 profiles of tibial cartilage, but a statistically significant decrease in T2 of the superficial 40% of weight-bearing femoral cartilage after exercise. These data support the hypothesis that cartilage compression results in greater anisotropy of superficial collagen fibers. Dunn et al. analyzed 55 subjects who were categorized with radiography as healthy ($n=7$) or as having mild OA ($n=20$) or severe OA ($n=28$) [56]. These authors found that healthy subjects had mean T2 values of 32.1–35.0 ms, while patients with mild and severe OA had mean T2 values of 34.4–41.0 ms. All cartilage compartments except the lateral tibia showed significant ($P<0.05$) increases in T2 relaxation time between healthy and diseased knees. The correlation of T2 values with clinical

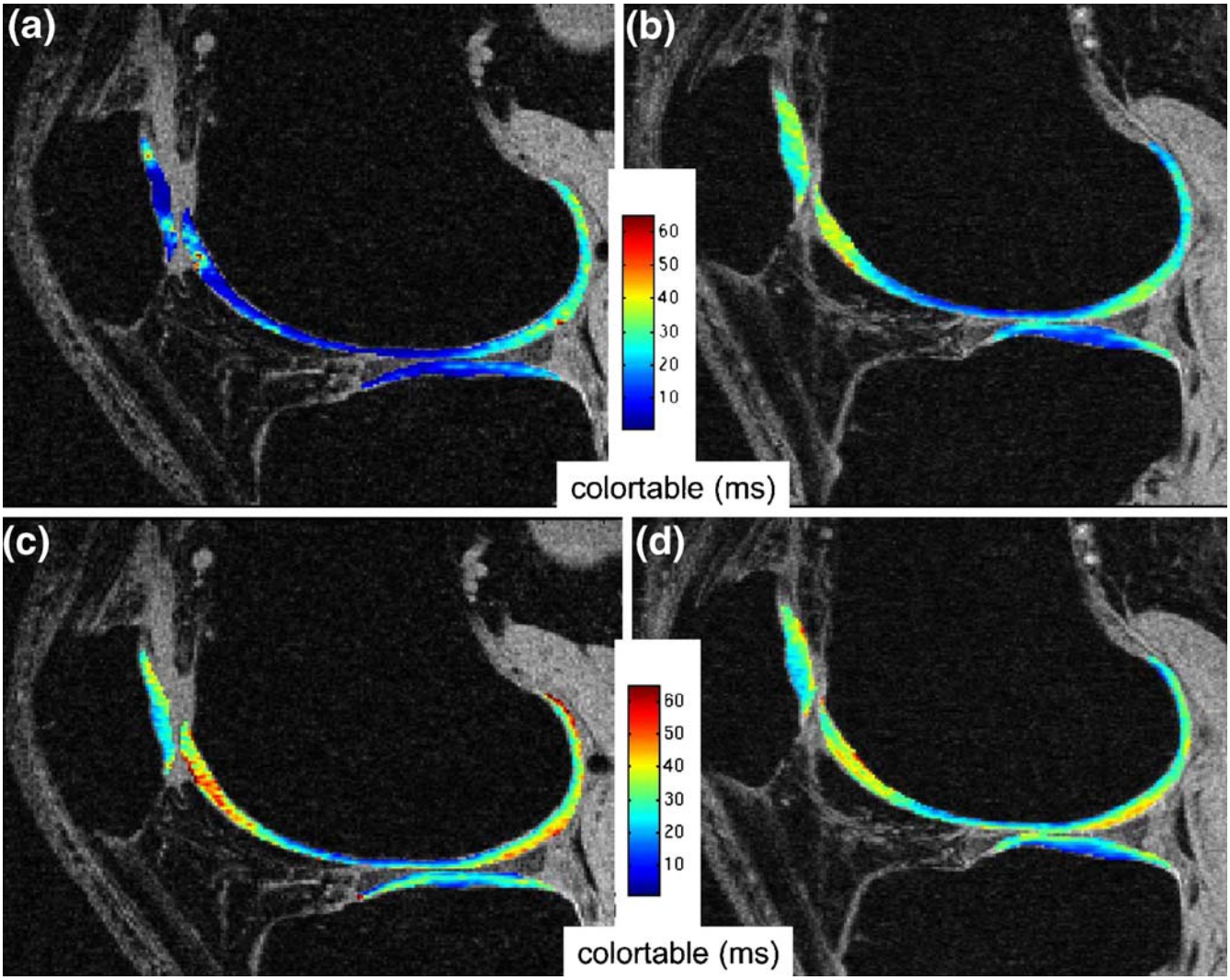

Fig. 12 Color-coded T2 (**a**, **b**) and T1rho (**c**, **d**) maps overlaid on a sagittal SPGR image in a 35-year-old male before (**a, c**) and after (**b, d**) a marathon. After the marathon (**b**), T2 times were significantly increased, mainly in the patella and the trochlea (from 14.4±15.01 ms to 35.2±7.71 ms), indicating cartilage edema with increased water content secondary to the physical stress. The patella, femur and lateral tibia plateau showed only a small increase in T1rho times after the marathon (**d**), indicating only a subtle change in cartilage macromolecular matrix

symptoms and cartilage morphology was found predominantly in medial compartments.

A different parameter that has been proposed to measure cartilage composition is 3D-T1rho-relaxation mapping (Fig. 12). T1rho describes the spin-lattice relaxation in the rotating frame, and changes in the extracellular matrix of cartilage, like the loss of GAG, may be reflected in measurements of T1rho due to less restricted motion of water protons. Preliminary results demonstrated the in vivo feasibility of quantifying early biochemical changes in symptomatic osteoarthritis subjects employing T1rho-weighted MR imaging on a 1.5-T clinical scanner [57, 58]. In a study with a limited number of symptomatic subjects, it was shown that T1rho-weighted MRI provided a noninvasive marker for quantitation of early degenerative changes of cartilage in vivo [57]. Li et al. examined ten healthy volunteers and nine osteoarthritis patients at 3T and found a significant difference (P=0.002) in the average T1rho within patellar and femoral cartilage between controls (45.04±2.59 ms) and osteoarthritis patients (53.06±4.60 ms) [59]. A significant correlation was found between T1rho and T2 relaxation measurements; however, the difference of T2 was not significant between controls and osteoarthritis patients. These initial results suggested that T1rho relaxation times may be a promising clinical tool for osteoarthritis detection and treatment monitoring. Further studies are clearly mandated to correlate T1rho measurements with early osteoarthritis determined from arthroscopy, as a standard of reference, in larger symptomatic populations [57].

A future technique to assess the structural properties of cartilage may be diffusion tensor imaging (DTI). DTI determines, in addition to T2 and T1rho mapping, not only the degree, but also the main direction of the free mobility of water protons. The findings from Filidoro et al. [60] on patella specimens at 9.4 T suggest that the DTI-derived parameter fractional anisotropy (FA) and eigenvector maps might reflect the macromolecular environment (like GAG concentration) and the predominant alignment of the collagenous fiber network, respectively. However, further studies are required to establish DTI at clinical high-field-strength systems for the use in human subjects.

Summary and conclusion

Recent new therapeutic modalities, in particular in osteoarthritis, have made cartilage MR imaging an exciting field of clinical interest and research. Cartilage imaging is a challenge, but new techniques provide better morphologic visualization and quantification as well as insights in the cartilage composition. It should be noted that currently morphologic imaging to depict cartilage lesions is standard for the clinical routine, and a number of cartilage dedicated sequences are available for this purpose. These, however, show damage at stages when cartilage is irreversibly lost. The future goal of MR imaging will be to diagnose cartilage matrix changes at stages when damage to the cartilage is still reversible and may be treated. This is an ambitious goal, yet promising tools, such as dGEMRIC, T1-rho and T2-relaxation time mapping are already available, and future research will show how clinically feasible these new biomarkers are as measures of early cartilage degeneration. Together with new pharmacological therapies, this may revolutionize management of osteoarthritis and could have a tremendous impact on population health. There is a huge interest in these MR techniques from other subspecialties, including rheumatologists and orthopedists; we as radiologists have to work hard to stay on top of this and keep up to date with the new developments.

References

1. Bentley G, Biant LC, Carrington RW, Akmal M, Goldberg A, Williams AM, Skinner JA, Pringle J (2003) A prospective, randomised comparison of autologous chondrocyte implantation versus mosaicplasty for osteochondral defects in the knee. J Bone Joint Surg Br 85:223–230
2. Cain EL, Clancy WG (2001) Treatment algorithm for osteochondral injuries of the knee. Clin Sports Med 20:321–342
3. Koulalis D, Schultz W, Heyden M, Konig F (2003) Autologous osteochondral grafts in the treatment of cartilage defects of the knee joint. Knee Surg Sports Traumatol Arthrose 12:329–334
4. Imhoff AB, Oettl GM (2000) Arthroscopic and open techniques for transplantation of osteochondral autografts and allografts in various joints. Surg Technol Int VIII:249–252
5. Hangody L (2003) The mosaicplasty technique for osteochondral lesions of the talus. Foot Ankle Clin 8:259–273
6. Link TM, Mischung J, Wortler K, Burkart A, Rummeny EJ, Imhoff AB (2006) Normal and pathological MR findings in osteochondral autografts with longitudinal follow-up. Eur Radiol 16:88–96
7. Kawasaki K, Uchio Y, Adachi N, Iwasa J, Ochi M (2003) Drilling from the intercondylar area for treatment of osteochondritis dissecans of the knee joint. Knee 10:257–263
8. James SL, Connell DA, Saifuddin A, Skinner JA, Briggs TW (2006) MR imaging of autologous chondrocyte implantation of the knee. Eur Radiol 16:1022–1030
9. Henderson IJ, Tuy B, Connell D, Oakes B, Hettwer WH (2003) Prospective clinical study of autologous chondrocyte implantation and correlation with MRI at 3 and 12 months. J Bone Joint Surg Br 85:1060–1066
10. Roberts S, McCall IW, Darby AJ, Menage J, Evans H, Harrison PE, Richardson JB (2003) Autologous chondrocyte implantation for cartilage repair: monitoring its success by magnetic resonance imaging and histology. Arthritis Res Ther 5:R60–R73
11. Horas U, Pelinkovic D, Herr G, Aigner T, Schnettler R (2003) Autologous chondrocyte implantation and osteochondral cylinder transplantation in cartilage repair of the knee joint A prospective, comparative trial. J Bone Joint Surg Am 85-A: 185–192
12. Fajardo M, Di Cesare PE (2005) Disease-modifying therapies for osteoarthritis: current status. Drugs Aging 22:141–161
13. Volpi N (2004) The pathobiology of osteoarthritis and the rationale for using the chondroitin sulfate for its treatment. Curr Drug Targets Immune Endocr Metabol Disord 4:119–127
14. Link TM, Sell CA, Masi JN, Phan C, Newitt D, Lu Y, Steinbach L, Majumdar S (2005) 3.0 vs 1.5T MRI in the detection of focal cartilage pathology-ROC analysis in an experimental model. Osteoarthr Cartil 14:63–70
15. Masi JN, Sell CA, Phan C, Han E, Newitt D, Steinbach L, Majumdar S, Link TM (2005) Cartilage MR imaging at 3.0 versus that at 1.5 T: preliminary results in a porcine model. Radiology 236:140–150
16. Yoshioka H, Stevens K, Hargreaves BA, Steines D, Genovese M, Dillingham MF, Winalski CS, Lang P (2004) Magnetic resonance imaging of articular cartilage of the knee: comparison between fat-suppressed three-dimensional SPGR imaging, fat-suppressed FSE imaging, and fat-suppressed three-dimensional DEFT imaging, and correlation with arthroscopy. J Magn Reson Imaging 20:857–864

17. Bredella MA, Tirman PF, Peterfy CG, Zarlingo M, Feller JF, Bost FW, Belzer JP, Wischer TK, Genant HK (1999) Accuracy of T2-weighted fast spin-echo MR imaging with fat saturation in detecting cartilage defects in the knee: comparison with arthroscopy in 130 patients. AJR Am J Roentgenol 172:1073–1080
18. Woertler K, Strothmann M, Tombach B, Reimer P (2000) Detection of articular cartilage lesions: experimental evaluation of low-and high-field-strength MR imaging at 0.18 and 1.0 T. J Magn Reson Imaging 11:678–685
19. Ruehm S, Zanetti M, Romero J, Hodler J (1998) MRI of patellar articular cartilage: evaluation of an optimized gradient echo sequence (3D-DESS). J Magn Reson Imaging 8:1246–1251
20. Kladny B, Gluckert K, Swoboda B, Beyer W, Weseloh G (1995) Comparison of low-field (0.2 Tesla) and high-field (1.5 Tesla) magnetic resonance imaging of the knee joint. Arch Orthop Trauma Surg 114:281–286
21. Vahlensieck M, Schnieber O (2003) [Performance of an open low-field MR unit in routine examination of knee lesions and comparison with high field systems]. Orthopade 32:175–178
22. Bauer J, Barr C, Steinbach L, Malfair D, Krug R, Ma C, Link T (2006) Imaging of the articular cartilage of the ankle at 3.0 and 1.5 Tesla. Eur Radiol Supplements 16 (S1):238
23. Gold GE, Han E, Stainsby J, Wright G, Brittain J, Beaulieu C (2004) Musculoskeletal MRI at 3.0 T: relaxation times and image contrast. AJR Am J Roentgenol 183:343–351
24. Gold GE, Suh B, Sawyer-Glover A, Beaulieu C (2004) Musculoskeletal MRI at 3.0 T: initial clinical experience. AJR Am J Roentgenol 183:1479–1486
25. Fischbach F, Bruhn H, Unterhauser F, Ricke J, Wieners G, Felix R, Weiler A, Schroder RJ (2005) Magnetic resonance imaging of hyaline cartilage defects at 1.5T and 3.0T: comparison of medium T2-weighted fast spin echo, T1-weighted two-dimensional and three-dimensional gradient echo pulse sequences. Acta Radiol 46:67–73
26. Kornaat PR, Reeder SB, Koo S, Brittain JH, Yu H, Andriacchi TP, Gold GE (2005) MR imaging of articular cartilage at 1.5 T and 3.0 T: comparison of SPGR and SSFP sequences. Osteoarthritis Cartilage 13:338–344
27. Hargreaves BA, Gold GE, Lang PK, Conolly SM, Pauly JM, Bergman G, Vandevenne J, Nishimura DG (1999) MR imaging of articular cartilage using driven equilibrium. Magn Reson Med 42:695–703
28. Gold GE, Fuller SE, Hargreaves BA, Stevens KJ, Beaulieu CF (2005) Driven equilibrium magnetic resonance imaging of articular cartilage: initial clinical experience. J Magn Reson Imaging 21:476–481
29. Hargreaves BA, Gold GE, Beaulieu CF, Vasanawala SS, Nishimura DG, Pauly JM (2003) Comparison of new sequences for high-resolution cartilage imaging. Magn Reson Med 49:700–709
30. Gagliardi JA, Chung EM, Chandnani VP, Kesling KL, Christensen KP, Null RN, Radvany MG, Hansen MF (1994) Detection and staging of chondromalacia patellae: relative efficacies of conventional MR imaging, MR arthrography, and CT arthrography. AJR Am J Roentgenol 163:629–636
31. Kramer J, Recht MP, Imhof H, Stiglbauer R, Engel A (1994) Postcontrast MR arthrography in assessment of cartilage lesions. J Comput Assist Tomogr 18:218–224
32. Woertler K, Rummeny EJ, Settles M (2005) A fast high-resolution multislice T1-weighted turbo spin-echo (TSE) sequence with a DRIVen equilibrium (DRIVE) pulse for native arthrographic contrast. AJR Am J Roentgenol 185:1468–1470
33. Raynauld JP, Martel-Pelletier J, Berthiaume MJ, Beaudoin G, Choquette D, Haraoui B, Tannenbaum H, Meyer JM, Beary JF, Cline GA, Pelletier JP (2005) Long term evaluation of disease progression through the quantitative magnetic resonance imaging of symptomatic knee osteoarthritis patients: correlation with clinical symptoms and radiographic changes. Arthritis Res Ther 8:R21
34. Raynauld JP, Martel-Pelletier J, Berthiaume MJ, Labonte F, Beaudoin G, de Guise JA, Bloch DA, Choquette D, Haraoui B, Altman RD, Hochberg MC, Meyer JM, Cline GA, Pelletier JP (2004) Quantitative magnetic resonance imaging evaluation of knee osteoarthritis progression over two years and correlation with clinical symptoms and radiologic changes. Arthritis Rheum 50:476–487
35. Blumenkrantz G, Lindsey CT, Dunn TC, Jin H, Ries MD, Link TM, Steinbach LS, Majumdar S (2004) A pilot, two-year longitudinal study of the interrelationship between trabecular bone and articular cartilage in the osteoarthritic knee. Osteoarthr Cartil 12:997–1005
36. Ghosh S, Ries M, Lane N, Ghajar C, Majumdar S (2000) Segmentation of high resolution articular cartilage MR images. Trans Orthoped Res Soc (ORS):246
37. Solloway S, Hutchinson CE, Waterton JC, Taylor CJ (1997) The use of active shape models for making thickness measurements of articular cartilage from MR images. Magn Reson Med 37:943–952
38. Stammberger T, Eckstein F, Michaelis M, Englmeier KH, Reiser M (1999) Interobserver reproducibility of quantitative cartilage measurements: comparison of B-spline snakes and manual segmentation. Magn Reson Imaging 17:1033–1042
39. Eckstein F, Heudorfer L, Faber SC, Burgkart R, Englmeier KH, Reiser M (2002) Long-term and resegmentation precision of quantitative cartilage MR imaging (qMRI). Osteoarthr Cartil 10:922–928
40. Burgkart R, Glaser C, Hyhlik-Durr A, Englmeier KH, Reiser M, Eckstein F (2001) Magnetic resonance imaging-based assessment of cartilage loss in severe osteoarthritis: accuracy, precision, and diagnostic value. Arthritis Rheum 44:2072–2077
41. Burgkart R, Glaser C, Hinterwimmer S, Hudelmaier M, Englmeier KH, Reiser M, Eckstein F (2003) Feasibility of T and Z scores from magnetic resonance imaging data for quantification of cartilage loss in osteoarthritis. Arthritis Rheum 48:2829–2835
42. Eckstein F, Charles HC, Buck RJ, Kraus VB, Remmers AE, Hudelmaier M, Wirth W, Evelhoch JL (2005) Accuracy and precision of quantitative assessment of cartilage morphology by magnetic resonance imaging at 3.0 T. Arthritis Rheum 52:3132–3136
43. Bauer J, S K, Ross C, Mueller D, Majumdar S, Link T (2005) Accuracy of volumetric cartilage measurements of the knee at 1.5 T and 3.0 T. In: RSNA, Chicago, p 305
44. Trattnig S, Mlynarik V, Breitenseher M, Huber M, Zembsch A, Rand T, Imhof H (1999) MRI visualization of proteoglycan depletion in articular cartilage via intravenous administration of Gd-DTPA. Magn Reson Imaging 17:577–583
45. Bashir A, Gray ML, Hartke J, Burstein D (1999) Nondestructive imaging of human cartilage glycosaminoglycan concentration by MRI. Magn Reson Med 41:857–865
46. Burstein D, Gray M (2003) New MRI techniques for imaging cartilage. J Bone Joint Surg Am 85-A Suppl 2:70–77

47. Gillis A, Bashir A, McKeon B, Scheller A, Gray ML, Burstein D (2001) Magnetic resonance imaging of relative glycosaminoglycan distribution in patients with autologous chondrocyte transplants. Invest Radiol 36:743–748
48. Williams A, Gillis A, McKenzie C, Po B, Sharma L, Micheli L, McKeon B, Burstein D (2004) Glycosaminoglycan distribution in cartilage as determined by delayed gadolinium-enhanced MRI of cartilage (dGEMRIC): potential clinical applications. AJR Am J Roentgenol 182:167–172
49. Williams A, Sharma L, McKenzie CA, Prasad PV, Burstein D (2005) Delayed gadolinium-enhanced magnetic resonance imaging of cartilage in knee osteoarthritis: findings at different radiographic stages of disease and relationship to malalignment. Arthritis Rheum 52:3528–3535
50. Woertler K, Buerger H, Moeller J, Rummeny EJ (2004) Patellar articular cartilage lesions: in vitro MR imaging evaluation after placement in gadopentetate dimeglumine solution. Radiology 230:768–773
51. Wiener E, Woertler K, Settles M, Rummeny E (2006) Quantification of T1 and T2 in the presence of Gd-DTPA of proteoglycan and collagen depleted cartilage. Eur Radiol (Suppl) 16:238
52. Liess C, Lusse S, Karger N, Heller M, Gluer CC (2002) Detection of changes in cartilage water content using MRI T2-mapping in vivo. Osteoarthr Cartil 10:907–913
53. Dardzinski BJ, Mosher TJ, Li S, Van Slyke MA, Smith MB (1997) Spatial variation of T2 in human articular cartilage. Radiology 205:546–550
54. Mosher TJ, Dardzinski BJ, Smith MB (2000) Human articular cartilage: influence of aging and early symptomatic degeneration on the spatial variation of T2–preliminary findings at 3 T. Radiology 214:259–266
55. Mosher TJ, Smith HE, Collins C, Liu Y, Hancy J, Dardzinski BJ, Smith MB (2005) Change in knee cartilage T2 at MR imaging after running: a feasibility study. Radiology 234:245–249
56. Dunn TC, Lu Y, Jin H, Ries MD, Majumdar S (2004) T2 relaxation time of cartilage at MR imaging: comparison with severity of knee osteoarthritis. Radiology 232:592–598
57. Regatte RR, Akella SV, Wheaton AJ, Lech G, Borthakur A, Kneeland JB, Reddy R (2004) 3D-T1rho-relaxation mapping of articular cartilage: in vivo assessment of early degenerative changes in symptomatic osteoarthritic subjects. Acad Radiol 11:741–749
58. Regatte RR, Akella SV, Borthakur A, Kneeland JB, Reddy R (2003) In vivo proton MR three-dimensional T1rho mapping of human articular cartilage: initial experience. Radiology 229:269–274
59. Li X, Han ET, Ma CB, Link TM, Newitt DC, Majumdar S (2005) In vivo 3-T spiral imaging based multi-slice T (1rho) mapping of knee cartilage in osteoarthritis. Magn Reson Med 54:929–936
60. Filidoro L, Dietrich O, Weber J, Rauch E, Oerther T, Wick M, Reiser MF, Glaser C (2005) High-resolution diffusion tensor imaging of human patellar cartilage: feasibility and preliminary findings. Magn Reson Med 53:993–998